

# MERLIN T4: PUSHING THE BOUNDARIES OF STEM/TEM WITH THE NEW TIMEPIX4 ASIC

Matúš Krajňák<sup>1\*</sup>, Gearóid Mangan<sup>1</sup>

<sup>1</sup>Quantum Detectors Ltd, R103 Rutherford Appleton Laboratory, Harwell Science & Innovation Campus, Harwell Oxford OX11 0QX, United Kingdom

\*matus@quantumdetectors.com

Merlin T4 from Quantum Detectors, based on the Timepix4 ASIC developed by the Medipix collaboration at CERN [1], is a next-generation hybrid pixel counting detector for transmission electron microscopy (TEM) that integrates and extends the capabilities of earlier ASIC generations within a single platform. It supports data-driven and frame-based operation. In data-driven mode, individual electron events are recorded with position (X, Y), time of arrival (ToA), and deposited energy (ToT), supporting beam currents up to 200 pA with 196 ps timing precision, while frame mode reaches up to 40k fps with 8-bit dynamic range across the full 512 x 448 pixel array.

This poster highlights the practical advantages of Merlin T4 for TEM applications. Data-driven acquisition enables fast 4D-STEM, correlative, diffraction, EELS, and dynamic TEM microscopy, while frame-based operation accommodates higher currents for nanobeam diffraction and dynamic TEM imaging. Sub-nanosecond timestamping combined with energy measurement further enhances detector performance and enables data volume reduction through post-processing. An example of imaging improvement is demonstrated for a single diffraction pattern in Fig. 1.

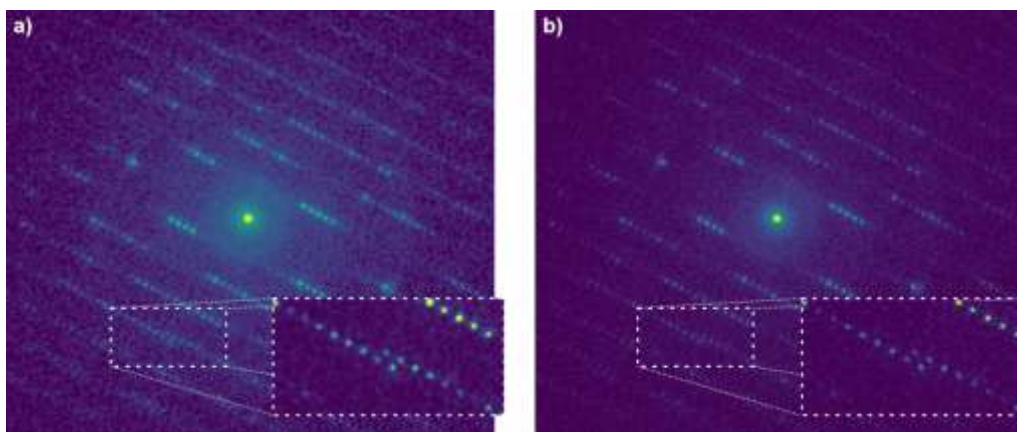


Fig. 1: Merlin T4 diffraction data improvement through post-processing: (a) raw frame; (b) reconstruction using local detector-response analysis and clustering. Main patterns are shown in logarithmic contrast; inset details are shown in linear contrast. Data were acquired on a JEOL cryoARM microscope (Crewe) at the Rosalind Franklin Institute with 200 kV beam energy; frames correspond to a 0.782 ms snapshot during continuous tilt of a biotin sample. [2]

## References:

[1] X. Llopart, et al., Journal of Instrumentation 17.01 C01044 (2022)

[2] Acknowledgements: Marcus Gallagher-Jones, Zhiyuan Ding, Angus Kirkland, Rosalind Franklin Institute

# Precession-enhanced Electric Field and Pair Distribution Function mapping in the Transmission Electron Microscope

Martijn Fransen<sup>1\*</sup>, Athanassios S. Galanis<sup>1</sup>, Alejandro Gomez-Perez<sup>1</sup>, Joaquim Portillo<sup>1</sup>, Evangelos Grivas<sup>1</sup>, Partha Pratim Das<sup>1</sup>, Stavros Nicolopoulos<sup>1</sup>

<sup>1</sup>NanoMEGAS, Rue Emile Claus 49 bte 9, 1050 Brussels, Belgium

\*martijn@nanomegas.com

The use of a precessing electron beam in 4DSTEM for improving the quality of diffraction patterns is well known in literature. The same methodology can also be applied for tackling other materials analysis problems such as the measurement of local fields in the sample [1] and the characterization of amorphous materials [2].

In this poster, we will demonstrate the advantages of using precession for electric field measurements, and describe how we aim to extend this application to the mapping of local magnetic fields. Additionally, we will show results on the automatic analysis of short-range order in amorphous materials from 4DSTEM maps using the electron Pair Distribution Function analysis, and present our roadmap on extending this capabilities towards amorphous phase mixtures and strained amorphous materials.

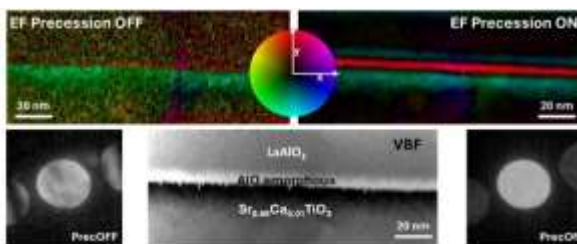


Fig. 1: Example of the benefits of precession in an e-field mapping experiment.

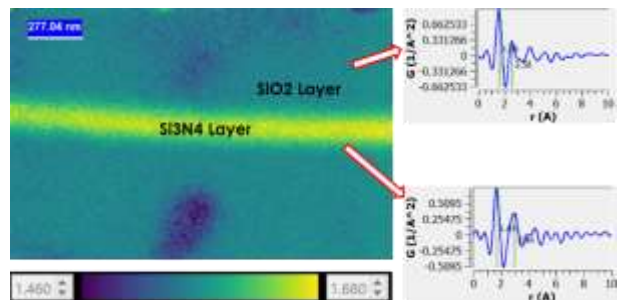


Fig. 2: Determination of short range order in a semiconductor device cross-section.

## References:

- [1] Y. Rakita et al. Acta Materialia 2023, **242**, 118426
- [2] S. Cao et al. et al. Proceedings of the IEEE International Symposium on Physical & Failure Analysis of Integrated Circuits, July 24-27, 2023

# Streamlined Software for 4D STEM Experiments and Real-Time Virtual Detector Calculation

Tia Truglas<sup>1\*</sup>, Marco Oster<sup>1</sup>, Dominic Tietz<sup>1</sup>, Max Krichenbauer and Hans Tietz<sup>1</sup>

<sup>1</sup>Tietz Video and Image Processing Systems GmbH, Ferdinand-Porsche-Str. 3, 82205 Gilching, Germany

\*tia.truglas@tvips.com

With its broad range of applications, 4D STEM is increasingly used as a standard technique. To minimize overhead and simplify usage, we developed EMplified Scan, a software package that supports 4D STEM acquisition with TVIPS TemCam-XF cameras and DECTRIS hybrid detectors, such as QUADRO and the ultra-fast ARINA detector. Synchronization of scanning and image acquisition is handled by the TVIPS Universal Scan Generator. The datasets are stored in lossless compressed HDF5 format with complete metadata for seamless postprocessing.

EMplified Scan enables real-time computation of virtual detectors, allowing multiple custom detectors to be displayed alongside standard STEM detectors during continuous acquisition. It also integrates essential microscope control functions, including automatic beam blanking and detector insertion/retraction.

Camera systems from TVIPS and from DECTRIS can be integrated into EMplified Scan, making it a flexible solution for upgrading JEOL or TFS microscopes with 4D STEM capability. Performance examples are:

- DECTRIS ARINA: 1024 × 1024 scan with 2× binned pixels (96 × 96 pixels) in <10 s.
- TVIPS TemCam-XF416ES: 100 x 100 scan at a camera format of 1024 x 1024 pixels in <1 min. It offers a large resolution and field of view of up to 4k x 4k pixels with a pixel size of 15.5 μm.

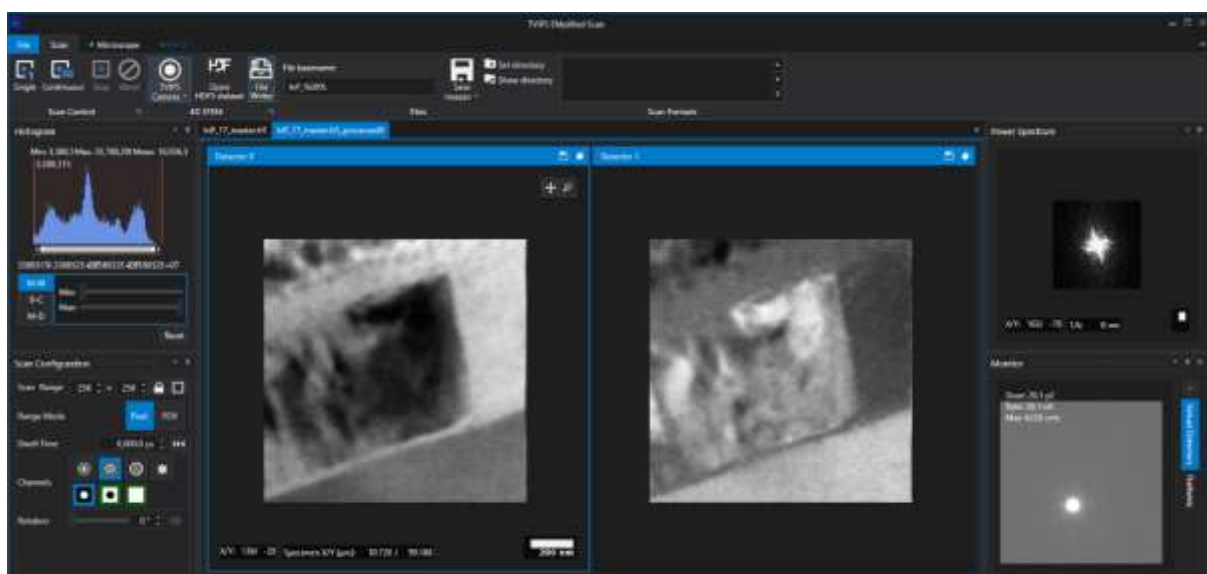


Fig. 1: Screenshot of EMplified Scan showing virtual dark and bright field detector images of a cross section of sputtered InP. The monitor image (right lower corner) shows the live diffraction pattern on a TemCam-XF416.

# AUTOMATED STAGE-ROCKED SCANNING PRECESSION ELECTRON DIFFRACTION IN AN SEM WITH AN ULTRAFAST EVENT-DRIVEN DETECTOR

Peng-Han Lu<sup>1\*</sup>, Chongzhi Zhu<sup>1</sup>, Dmitry Byelov<sup>2</sup>, Dima Nikolaiev<sup>2</sup>, Walter van Bodegom<sup>2</sup>, Fabian Perez Willard<sup>3</sup>, Bjoern Gamm<sup>3</sup>, Pascal M. Anger<sup>3</sup>, Xiong Liu<sup>3</sup>, Lei Jin<sup>1</sup>, Rafal E. Dunin-Borkowski<sup>1</sup>

<sup>1</sup>Forschungszentrum Jülich, Ernst-Ruska Centre for Microscopy and Spectroscopy with Electrons, Wilhelm-Johnen-Straße, 52425, Jülich, Germany

<sup>2</sup>Amsterdam Scientific Instruments, Science Park 106, 1098 XG, Amsterdam, Netherlands

<sup>3</sup>Carl Zeiss Microscopy GmbH, Carl-Zeiss-Straße 22, 73447, Oberkochen, Germany

\*p.lu@fz-juelich.de

Scanning precession electron diffraction (SPED) measures a series of spatially-resolved transmission electron diffraction patterns with a precessed, nanometer-sized electron probe scanning over a specimen. Featured by double conical beam rocking [1], this approach suppresses dynamic diffraction effects and offers accurate orientation mapping, phase identification and strain analysis in crystalline materials. Here we replace the pre- and post-specimen beam rocking by a stage rocking and implement an automated SPED workflow in a scanning electron microscope (SEM) with an ultrafast event-driven detector. The detector is attached to the SEM stage for its own manoeuvre, while a hexapod-like rocking stage is added on top of the SEM stage (Fig. 1) so that the specimen can be positioned independently, oriented to desired crystallographic axis, and tilted to different azimuthal angles. Two different camera lengths of around 75 mm and 125 mm are accessible. The detector consists of 2x2 Timepix3 chips (in total 512x512 pixels) with maximal permitted event rate up to 320 Mhit/s. This allows effectively MHz frame rate with reasonable probe current and facilitates serial measurements at different stage azimuthal tilting angles, which can be post-merged into a SPED dataset. The developed SPED-in-SEM workflow offers high-throughput reliable orientation/phase mapping in more accessible SEM platforms, but also allows FIB-prepared specimen directly characterized in the same vacuum chamber without exposed to air and transfer to a TEM, especially important for air-sensitive specimens.

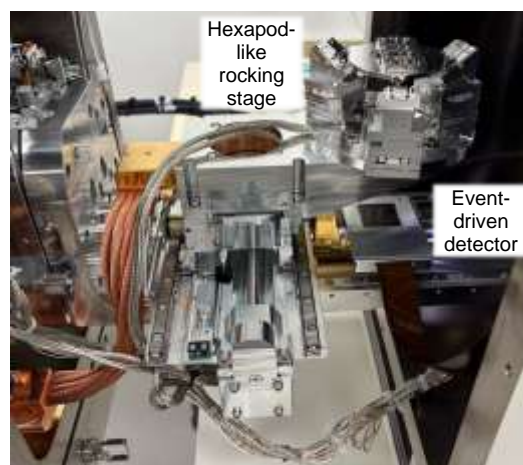


Fig. 1: This is an image

## References:

[1] R. Vincent & P.A. Midgley, *Ultramicroscopy* **53**, 271-282 (1994).

# Fourier precession TEM applied to dose-sensitive biological samples

Maiko Czarnetzki<sup>1\*</sup>, Tizian Lorenzen<sup>2</sup>, Daniel Mann<sup>1</sup>,  
Knut Müller-Caspary<sup>2</sup> and Carsten Sachse<sup>1,3</sup>

<sup>1</sup>Forschungszentrum Jülich, Ernst Ruska Centre 3, Wilhelm Johnen Straße 52428 Jülich, Germany

<sup>2</sup>Ludwig Maximilian Universität München, Department of Chemistry, Butenandstr. 11, 81377 Munich, Germany

<sup>3</sup>Heinrich Heine Universität Düsseldorf, Mathematisch-Naturwissenschaftliche Fakultät,  
Universitätsstraße 1, 40225 Düsseldorf Germany

\*m.czarnetzki@fz-juelich.de

Electron microscopes can be operated in different modes like conventional transmission electron microscopy (CTEM) and scanning TEM (STEM). CTEM in particular for observing cryo-vitrified specimens is well developed and offers advantages like a larger field of view, high-throughput data acquisition. However, in CTEM a range of defocus is used in order to increase phase contrast for biological samples, leading to information loss and complicating image interpretation. In STEM, phase contrast can be obtained by increasing the dimensionality of the dataset from 2D to 4D using differential phase contrast (DPC) or center-of-mass (COM) imaging. These imaging methods are still limited by the detector technology. While the pixelated detector is comparably slow, the segmented detector is limited in the number of available segments. By employing the reciprocity theorem, which relates both CTEM and STEM through a source-detector interchange, the advantages of both methods can be combined. Instead of acquiring TEM along the optical axis, the beam is tilted to a polar angle  $\theta$  and rotated over an azimuthal angle  $\varphi$  resulting in a sparse 4D-TEM dataset. This acquisition can be implemented with a continuously moving beam (precession) or by a discretely tilted beam. It has already been shown that Fourier-precession can enable direct mapping of built-in electric fields in nanostructures like the electric field in a GaAs p-n junction [1]. Here, the goal is to apply this method to dose-sensitive biological samples embedded in vitreous ice, specifically tobacco mosaic virus (TMV) that provides a highly symmetrical, helically ordered specimen that gives rise to characteristic layer lines in the FFT. The achievable resolution and contrast improvement by this method is assessed in this work by optimizing the acquisition set up as well as the subsequent reconstruction.

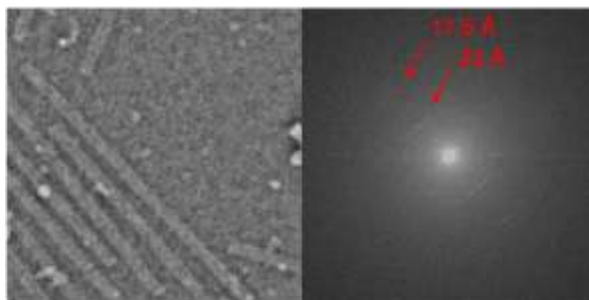


Fig. 1: Reconstructed iCOM from 8 discrete tilts at 4.8 mrad showing vitrified TMV rods and the respective FFT with layer lines visible at 23 and 11.5 Å.

## References:

[1] Lorenzen, T. *et al.* (2024) "Imaging built-in electric fields and light matter by Fourier-precession TEM," *Scientific Reports*, 14(1). <https://doi.org/10.1038/s41598-024-51423-x>

# Practical Challenges and Strategies for Phase Contrast 4D-STEM Tomography of Thick Biological Specimens

Berk Küçükoğlu<sup>1,2,3\*</sup>, Massimo Kube<sup>1,2</sup>, Wen-Lu Chung<sup>1,2</sup>, Georgios Varnavides<sup>10</sup>, Max Leo Leidl<sup>4,5</sup>, Abraham Lewis Levitan<sup>6,7</sup>, Julika Radecke<sup>1,2</sup>, Daniel Stähli<sup>1,2</sup>, Stephanie Ribet<sup>8</sup>, Carsten Sachse<sup>4</sup>, Manuel Guizar-Sicairos<sup>6,7</sup>, Colin Ophus<sup>9</sup>, Knut Müller-Caspary<sup>5</sup>, Henning Stahlberg<sup>1,2</sup>

<sup>1</sup>EPFL, LBEM, Institute of Physics, Route de la Sorge, 1015 Lausanne, Switzerland

<sup>2</sup>UNIL, Dept. of Fundamental Microbiology, Route de la Sorge, 1015 Lausanne, Switzerland

<sup>3</sup>DECTRIS AG, Taefernweg 1, 5405 Baden-Dättwil, Switzerland

<sup>4</sup>Forschungszentrum Jülich, ER-C-3: Structural Biology, Jülich, Germany

<sup>5</sup>LMU München, Dept. of Chemistry and Centre for NanoScience, Butenandstr. 11, 81377 München, Germany

<sup>6</sup>EPFL, Computational X-ray Imaging Laboratory, Route de la Sorge, 1015 Lausanne, Switzerland

<sup>7</sup>Paul Scherrer Institute, Forschungsstrasse 111, 5232 Villigen, Switzerland

<sup>8</sup>NCEM, Molecular Foundry, Lawrence Berkeley National Laboratory, Berkeley, CA 94720, USA

<sup>9</sup>Stanford University, Dept. of Materials Science and Engineering, Stanford, CA, USA

<sup>10</sup>Department of Imaging Physics, Delft University of Technology, Lorentzweg 1, 2628 CJ Delft, the Netherlands

\*berk.kucukoglu@dectris.com

4D-STEM combined with phase retrieval shows promise for tomographic imaging of thick biological specimens, where conventional cryo-EM is limited by inelastic and multiple scattering [1]. We collected 4D-STEM tilt series from specimens 200–700 nm thick, comparing ptychographic [2] and tilt-corrected bright-field STEM (tcBF/parallax) [3] reconstructions [4].

Several practical challenges arose during these reconstructions. Specimen tilt introduces a varying defocus across the field of view, which without dynamic defocusing during acquisition must be corrected computationally, either by choosing a single optimal defocus for parallax, or by varying the probe defocus as a function of scan position in the ptychographic forward model. Both approaches improve reconstruction quality but have limited effectiveness at high tilt angles, where hardware-level defocus correction becomes necessary. Additionally, multi-slice ptychography, despite its theoretical advantages [2], converged inconsistently at the single-digit  $e^-/\text{Å}^2$  doses typical of cryo-tomography. Parallax proved more robust under these conditions and yielded tomograms from which preliminary sub-tomogram averaging shows encouraging results. We discuss strategies to address these challenges.



Fig. 1: Projection from the tilt series, showing microtubules and gold fiducials.

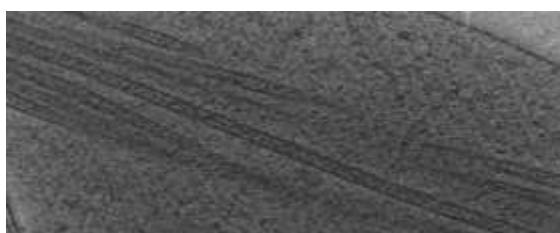


Fig. 2: Central slice of the tomogram reconstructed from the tilt series.

## References:

[1] Egerton RF. *Micron* (2024) 177, 103576.

[2] Chen Z et al. *Science* (2021) 372, 826–831.

[3] Yu Y et al. *bioRxiv* (2024) 2024.04.22.590491.

[4] Küçükoğlu B et al. *Microsc. Microanal.* (2025) 31(7), 2289–2290.

# DISTORTION CORRECTION IN MULTI-FRAME STEM

Pavel Potapov<sup>1,2\*</sup>, Giulio Guzzinati<sup>3</sup>

<sup>1</sup>IFW-Dresden, IFF, Helmholtzstr. 20, D-01069, Dresden, Germany

<sup>2</sup>TEM DM, am Grünen Grund 1, D-01109, Dresden, Germany

<sup>3</sup>CEOS GmbH, Englerstr. 28, D-69126, Heidelberg, Germany

\*pavel@temdm.com

STEM images suffer from distortions caused by sample drift and instabilities of the scan generator. These distortions are particularly pronounced in STEM spectrum-images, which typically require a longer dwell time. Multi-frame acquisition helps to mitigate these effects. Still, the following hierarchical strategy to correct STEM distortions is needed:

1. **Rigid frame alignment** via cross- or phase- correlation.
2. **Correction for continuous linear drift**, estimated from the rigid shifts between frames. Each frame is then corrected using the affine transformation that accounts for shear and contraction / extension. This transformation requires estimation of two free parameters.
3. **Correction for non-linear intra-frame oscillations**. After [1], we assume that distortions are negligible within each line along the fast-scan direction, while certain x/y shifts among rigid scan lines are allowed (Fig. 1a). The evaluation proceeds in two steps (Fig. 1b). First, we divide an image into representative horizontal stripes and compute cross-correlations with the corresponding stripes in a reference image. Second, we interpolate the resulted sparse shift points using a smooth cubic spline. The forthcoming back-mapping deforms the image toward the reference. Typically, several back-mapping iterations are required. This procedure can be applied to both multi-frame STEM images and spectrum-images, provided that the latter are accompanied by STEM HAADF acquisition. The correction requires an appropriate reference. For STEM spectrum-images, a fast-scanned overview image is suitable, as it efficiently reduces distortions of the slow-scanned spectrum-images to the level of the fast-scanned overview. If a higher accuracy of correction is required (e.g., multi-frame STEM imaging at moderate scan rates), two options for a reference are available: (i) an additional fast, noisy STEM image, or (ii) a frame with a minimal shift relative the other ones (Fig. 2).

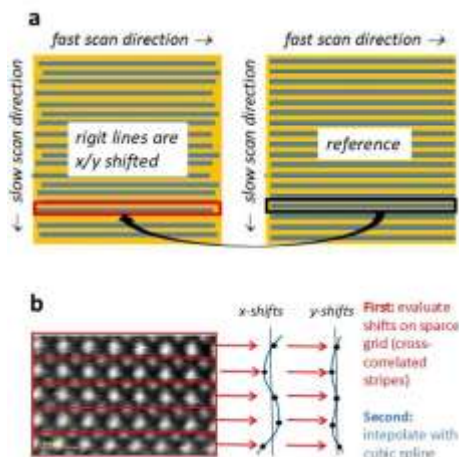


Fig. 1: (a) 'Rigid lines' approach and (b) stripe cross-correlation + interpolation method for evaluation of shifts.

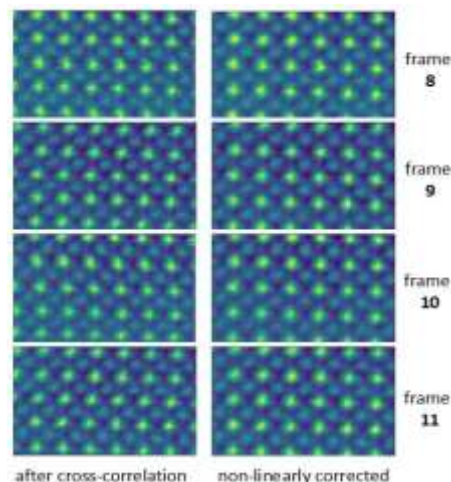


Fig. 2: Non-linear correction of multi-frame STEM. Step (2) was omitted. Step (3) was performed with a 'minimal-shift frame' as a reference.

Reference:

[1] C.Ophus, J.Ciston, C.T. Nelson, Ultramicroscopy **162**, 1-9 (2016).

# Peak-Preserving Denoising of 4D-STEM Diffraction Using Autoencoders

Karina Ruzaeva<sup>1\*</sup>, Dieter Weber<sup>2</sup>, Juri Barthel<sup>2</sup>, Matthew Bryan<sup>3</sup>, Bashir Kazimi<sup>1</sup>, Stefan Sandfeld<sup>1</sup>

<sup>1</sup>Institute for Advanced Simulations - Materials Data Science and Informatics (IAS-9),  
Forschungszentrum Jülich GmbH, 52428 Jülich, Germany

<sup>2</sup>Ernst Ruska-Centre for Microscopy and Spectroscopy with Electrons, Forschungszentrum Jülich GmbH,  
52428 Jülich, Germany

<sup>3</sup>Univ. Grenoble Alpes, CEA, Leti, F-38000 Grenoble, France

\*k.ruzaeva@fz-juelich.de

Four-dimensional scanning transmission electron microscopy (4D-STEM) enables spatially resolved crystallographic analysis of phase-change memory (PCM) devices during electrical switching [1], but the low electron dose required for in-situ measurements results in diffraction patterns with limited signal-to-noise ratio. Information relevant for phase and orientation mapping is encoded in weak, localized diffraction peaks [2], making reconstruction quality poorly captured by global similarity measures commonly used to train and evaluate autoencoders [3].

This work focuses on loss design and evaluation for autoencoder-based reconstruction of diffraction data. We introduce a signal-weighted reconstruction loss that explicitly accounts for the strongly inhomogeneous intensity distribution of diffraction patterns and increases sensitivity to weak non-zero-order reflections. To assess reconstruction fidelity in a manner aligned with crystallographic analysis, we further propose peak-based evaluation metrics that quantify peak localization accuracy and relative intensity consistency rather than pixel-wise agreement.

The approach is validated using synthetic diffraction datasets with known ground truth spanning multiple sparsity and length-scale regimes and is applied to experimental 4D-STEM data acquired from PCM devices. Compared to standard reconstruction objectives, the proposed loss improves retention of weak diffraction peaks and reduces spurious peak detections as measured by the proposed metrics. The low-dimensional latent representation also provides an efficient encoding of large 4D-STEM datasets, enabling substantial data reduction while preserving analysis-relevant information [4] and maintaining weak diffraction features in low-dose 4D-STEM measurements.

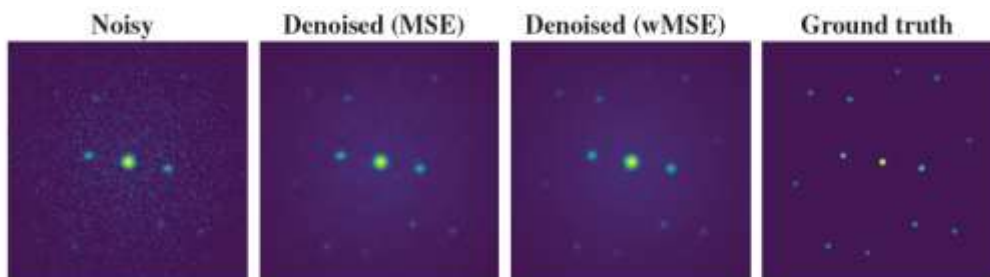


Fig. 1: Qualitative comparison of denoising results

## References:

- [1] C. Ophus, *Microscopy and Microanalysis* 25(3), 563–582 (2019).
- [2] E.F. Rauch, L. Dupuy, *Archives of Metallurgy and Materials* 50, 87–99 (2005).
- [3] L. Gondara, *IEEE International Conference on Data Mining Workshops (ICDMW)*, 241–246 (2016).
- [4] P. Akyazi, T. Ebrahimi, *IEEE/CVF Conference on Computer Vision and Pattern Recognition Workshops (CVPRW)* (2019).

# MAXIMUM A POSTERIORI DENOISING FOR 4D-STEM DATASET VIA TENSOR SPARSITY REGULARIZATION

Chongzhi Zhu<sup>1\*</sup>, Peng-Han Lu<sup>1</sup>, Lei Jin<sup>1</sup>, Rafal E. Dunin-Borkowski<sup>1</sup>

<sup>1</sup>Forschungszentrum Jülich, Ernst Ruska-Centre for Microscopy and Spectroscopy with Electrons, Wilhelm-Johnen-Straße, 52428, Jülich, Germany

\*c.zhu@fz-juelich.de

Four-dimensional scanning transmission electron microscopy (4D-STEM) offers promising imaging modes for probing beam-sensitive materials at ultra-low electron doses. However, the resulting 4D-STEM datasets are often degraded by mixed Poisson-Gaussian noise, which substantially limits their interpretability. We present a denoising framework that integrates: (i) an Improved Maximum A Posteriori (IMAP) noise model for statistically rigorous exit-wave refinement [1]; (ii) periodic block matching that exploits crystallographic lattice periodicity using a Kullback-Leibler divergence similarity metric [2]; and (iii) Kronecker-Basis Representation (KBR) tensor regularization to promote structured sparsity [3].

The IMAP model defines the data fidelity term via a weighted least squares objective that accounts for heteroscedastic counting noise under low-dose electron detection, together with additive Gaussian electronic noise. Periodic block matching leverages translational symmetry to group diffraction patterns from crystallographically equivalent positions, maximizing self-similarity while preserving detector coordinate structure critical for reciprocal-space relationships. KBR regularization combines core tensor sparsity with mode-wise low-rank structure through a log-sum relaxation, effectively unifying advantages of Tucker and Canonical polyadic decompositions [4]. Together, these components enforce fidelity to the mixed noise statistics while promoting physically meaningful, structured tensor representations.

By integrating physics-based noise modeling, crystallographic geometric priors, and advanced tensor regularization, the proposed approach is expected to deliver improved restoration on crystalline samples while maintaining physical consistency, including intensity conservation, positivity, and reciprocal space alignment.

## References:

- [1] Q. Xie *et al.* IEEE Trans. Med. Imag. **36**, 2487-2498 (2017).
- [2] N. Mevenkamp *et al.* Adv. Struct. Chem. Imaging **1**, 3 (2015).
- [3] Q. Xie *et al.* IEEE Trans. Pattern Anal. Mach. Intell. **40**, 1888-1902 (2018).
- [4] T.G. Kolda & B.W. Bader. SIAM Rev. **51**, 455-500 (2009).

# HIGH-THROUGHPUT, GENERAL-PURPOSE ELECTRON PTYCHOGRAPHY VIA STATISTICAL DEEP LEARNING

Han Yue<sup>1</sup>, Chien-Chun Chen<sup>2\*</sup>, Jun Cheng<sup>3</sup>, Steve F. Shu<sup>4</sup>

<sup>1</sup>Fudan University, College of Intelligent Robotics and Advanced Manufacturing,  
No. 220 Handan Road, 200433, Shanghai, China

<sup>2</sup>National Tsing Hua University, Department of Engineering and System Science,  
No. 101, Section 2, Kuang-Fu Road, 300044, Hsinchu, Taiwan

<sup>3</sup>Agency for Science, Technology and Research (A\*STAR), Institute for Infocomm Research,  
1 Fusionopolis Way, 138632, Singapore, Singapore

<sup>4</sup>The University of Sydney, School of Electrical and Computer Engineering, Building J03,  
Maze Crescent, NSW 2006, Sydney, Australia

\*chenchienchun0627@gmail.com

Electron ptychography routinely achieves sub-ångström spatial resolution, yet its application to high-throughput materials characterization is bottlenecked by the computational cost of iterative solvers. Conventional algorithms, such as the Extended Ptychographic Iterative Engine (ePIE), rely on sample-specific global optimization, which necessitates repetitive, time-consuming computation for every new field of view. Here, we present a deep learning framework designed to transcend these limitations, establishing a pathway for real-time, general-purpose phase imaging.

Distinguished from standard end-to-end surrogates that often overfit to specific structural templates, our framework is designed to approximate the intrinsic statistical mapping between diffraction intensities and phase shifts. By targeting fundamental scattering features rather than macroscopic object morphologies, the model exhibits remarkable robustness across varying specimen structures under a consistent instrument configuration. We validated the framework using experimental 4D-STEM datasets, demonstrating that a single trained model can reconstruct diverse atomic features with fidelity comparable to iterative solvers (Fig. 1). Frequency domain analysis confirms that the method strictly preserves the physical resolution limit and correctly reproduces medium-range order. In terms of efficiency, the inference process accelerates reconstruction by orders of magnitude compared to iterative baselines, matching the throughput of modern high-speed detectors and enabling continuous, large-scale atomic characterization without the need for repetitive per-scan optimization.

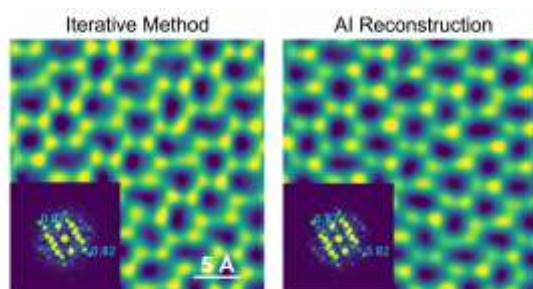


Fig. 1: Comparison of reconstruction fidelity and resolution

## References:

[1] J. Miao, *Nature* **637**, 281–295 (2025).

[2] H. Yue et al., *IEEE Transactions on Computational Imaging* **11**, 888–900 (2025).

# Design of a foil-lens spherical aberration corrector for SEM

Martin Vodička<sup>a,b</sup>, Ondřej L. Sháněl<sup>a,c</sup>, Radovan Vašina<sup>c</sup>

<sup>a</sup>*Institute of Physical Engineering, Brno University of Technology, Brno, Czech Republic*

<sup>b</sup>*Ernst Ruska-Centre for Microscopy and Spectroscopy with Electrons, Forschungszentrum Jülich GmbH, 52428, Germany*

<sup>c</sup>*Thermo Fisher Scientific, Brno, Czech Republic*

Contact email: 216935@vutbr.cz

In 1936, Otto Scherzer proved that static, rotationally symmetric electromagnetic lenses with zero on-axis charge inevitably exhibit positive spherical (Cs) and chromatic (Cc) aberrations [1]. This fundamental limitation has shaped electron optical design for nearly a century. One route to overcoming Scherzer's constraint is to violate its assumptions by introducing a charged element along the optical axis. A thin charged foil provides such a mechanism, enabling negative contributions to the spherical aberration coefficient through the fourth derivative of the axial electrostatic potential [2]:

$$C_s = \frac{1}{2\Phi_i^{1/2}r_\alpha^{14}(z_i)} \int_{z_o}^{z_i} \Phi^{1/2} \left\{ \left[ r_\alpha'^2 + \frac{\Phi''}{4\Phi} r_\alpha^2 \right]^2 - \frac{\Phi^{(4)}}{16\Phi} r_\alpha^4 \right\} dz.$$

As expressed by the formula, spherical aberration depends on both the axial potential distribution and the paraxial ray trajectory. However, modifying the potential alters the paraxial properties of the system itself, leading to strong internal interdependence between field configuration and ray propagation. This coupling complicates prediction of the achievable correction strength and raises a fundamental question: how can the correction power of a foil-based corrector be determined in a self-consistent and practical manner?

Here, we present a systematic analysis of a conceptually simple foil-corrector design (Fig. 1). We quantify its achievable correction strength, analyze stability and sensitivity, and evaluate its influence on system resolution and aperture angle control. Rather than focusing solely on minimizing Cs, we assess performance using practical implementation criteria, including robustness, tunability, and design simplicity.

Our results clarify the correction mechanisms enabled by charged foils and identify design principles for stable and effective operation. The proposed architecture represents a promising route toward compact, cost-effective, and user-accessible spherical aberration correction in electron optical systems.

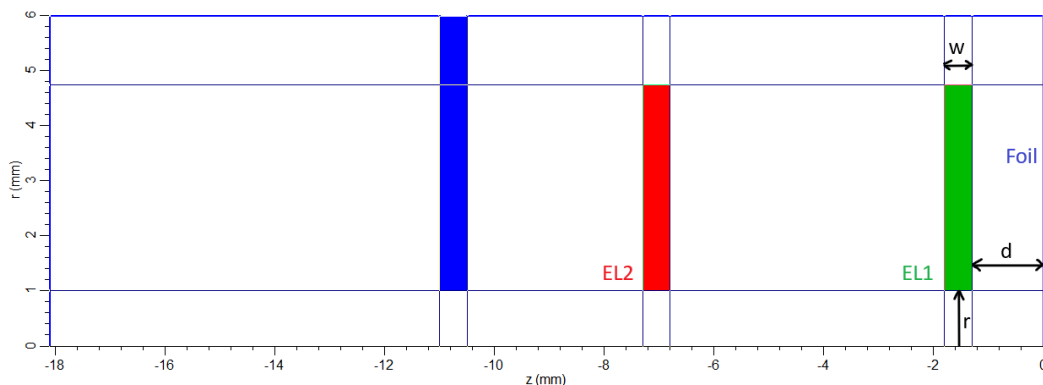


Figure 1 Design of a simple corrector system with foil-lens.

## References:

- [1] Scherzer, O. *Zeitschrift für Physik*. **1936**, vol. 10. doi: 10.1007/BF01349606.
- [2] van Aken et al., *Nucl. Instrum. Methods Phys. Res. A* 519 (2004) 205–215.

# AUTOMATED ANALYSIS OF STEM DATA OF SEMICONDUCTOR HETEROSTRUCTURES FOR QUANTUM COMPUTING

Marc Botifoll<sup>1\*</sup>, Ivan Pinto-Huguet<sup>1</sup>, Enzo Rotunno<sup>2</sup>, Thomas Galvani<sup>1</sup>, Catalina Coll<sup>1</sup>, Yann-Michel Niquet<sup>3</sup>, Sara Martí-Sánchez<sup>1</sup>, Georgios Katsaros<sup>4</sup>, Giordano Scappucci<sup>5</sup>, Peter Krogstrup<sup>6</sup>, Giovanni Isella<sup>7</sup>, Maria Chiara Spadaro<sup>1</sup>, Stephan Roche<sup>1,8</sup>, Pablo Ordejón<sup>1</sup>, Vincenzo Grillo<sup>2</sup>, Jordi Arbiol<sup>1,8</sup>

<sup>1</sup>ICN2, CSIC and BIST, Barcelona, Spain

<sup>2</sup>CNR-IMEM, Parma, Italy

<sup>3</sup>Univ. Grenoble Alpes, CEA, IRIG-MEM-L Sim, Grenoble, France

<sup>4</sup>Institute of Science and Technology Austria, Klosterneuburg, Austria

<sup>5</sup>QuTech and Kavli Institute of Nanoscience, Delft TU, Delft, The Netherlands

<sup>6</sup>10NNF Quantum Computing Programme, NBI, University of Copenhagen, Denmark

<sup>7</sup>Politecnico di Milano, Como, Italy

<sup>8</sup>ICREA, Barcelona, Catalonia, Spain

\*m.botifoll@fz-juelich.de

The process of discovering and refining new materials, as well as enhancing existing ones for a variety of uses, including quantum applications, is a complex and multifaceted endeavor. [1,2] We introduce an advanced analytical framework for the quantitative characterization of semiconductor and quantum heterostructures at the atomic scale. The methodology combines high-resolution Transmission Electron Microscopy (HR-TEM), Scanning TEM (STEM), and Electron Energy Loss Spectroscopy (EELS) to extract structural and compositional information with nanometric to sub-angstrom precision. The proposed workflow integrates conventional image analysis algorithms with both supervised and unsupervised machine learning procedures, enabling automated identification of material composition, crystallographic phase, and lattice orientation through direct model comparison. Beyond structural identification, the framework incorporates automated strain mapping and defect quantification, providing a comprehensive insight into nanoscale structural distortions that modulate device performance. The extracted parameters are used to generate physically consistent models for simulation, bridging experimental data with predictive computational tools to relate microstructural attributes to functional behavior. [3]

We demonstrate the approach on SiGe quantum well heterostructures optimized for spin qubit generation, among many other relevant materials science systems, achieving fully autonomous quantification of strain distribution and interfacial ordering. The workflow, however, is material-agnostic and scalable to a wide variety of heterostructured devices. Its generalization capability represents a significant advancement toward automated, reproducible, and model-integrated (S)TEM characterization for next-generation quantum and electronic device architectures.

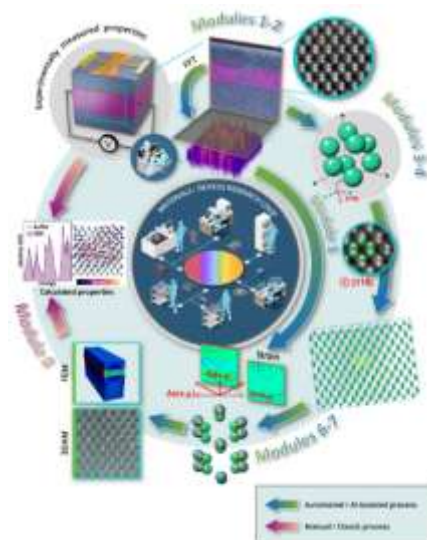


Figure 1: Automated workflow pipeline for the autonomous unveiling of physical knowledge.

## References:

- [1] Jirovec, D. et al. *Nature Materials*, (2021) doi.org/10.1038/s41563-021-01022-2
- [2] Paquelet, B. et al *Nat. Commun.* 14, 1385 (2023)
- [3] Botifoll, M. et al, *Adv. Mater.* (2025): e06785, <https://doi.org/10.48550/arXiv.2411.01024>

# QUANTITATIVE DETERMINATION OF STRAIN AND POLARIZATION FIELDS IN SEMICONDUCTOR HETEROSTRUCTURES USING PRECESSION-ASSISTED 4D-STEM

Yucheng Zou<sup>1\*</sup>, Lei Jin<sup>1</sup>, Peng-Han Lu<sup>1</sup>, Rafal E. Dunin-Borkowski<sup>1</sup>

<sup>1</sup>Forschungszentrum Jülich, Ernst-Ruska Centre for Microscopy and Spectroscopy with Electrons, Wilhelm-Johnen-Straße, 52425, Jülich, Germany

\*y.zou@fz-juelich.de

Precise quantification of internal electric fields and strain at semiconductor heterointerfaces is crucial for optimizing device functionality. Here, four-dimensional scanning transmission electron microscopy (4D-STEM) combined with fast beam precession is employed to reliably map strain and internal electric field distributions across AlGaIn-based heterostructures with nanoscale spatial resolution. The contribution of mean inner potential and polarization to the total electric fields were fitted, respectively, to the first derivative and linear component of the composition profile [1] (Fig. 1). Based on the chemical composition (determined by EDS) as well as the strain in each heterostructure layer, the spontaneous and piezoelectric polarization fields can be theoretically calculated and compared with the experimentally determined total polarization fields. The synergetic measurement and correlative analysis developed here provides direct insight into the interplay between local structure, composition, strain and polarization fields in semiconductor devices.

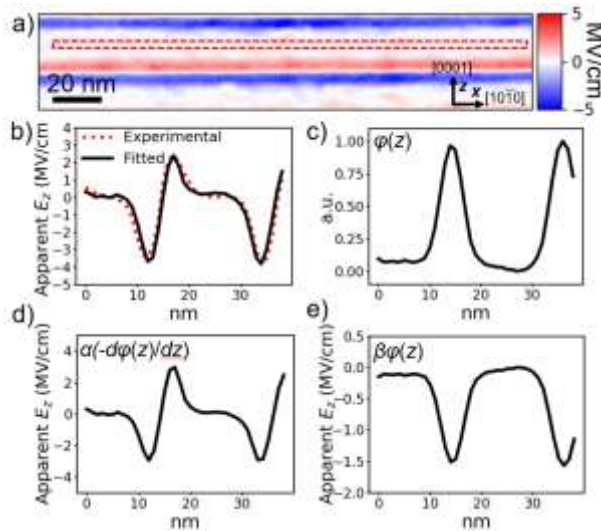


Fig. 1: a) Electric field map determined from the 4D-STEM dataset. b) Horizontally averaged line profile along the vertical direction from bottom to top in (a). The red dashed area in a) is chosen as the reference (zero value). c) Normalized composition profile determined from HAADF image intensity. d) Contribution of mean inner potential to the total electric fields fitted as the negative first derivative of the composition profile. e) Contribution of polarization to the total electric fields fitted as the linear component of composition profile.

References:

[1] K. Müller-Caspary *et al.* Physical Review Letters **122**, 106102 (2019).

# ULTRAFAST 4D-STEM – AN ULTRASENSITIVE PROBE OF NANO-PLASMA DYNAMICS

Nicolai-Leonid Bathen<sup>1,2\*</sup>, Michael Yannai<sup>1</sup>, Vasily A. Lebedev<sup>3</sup>, Rotem Elimelech<sup>1</sup>, Tal Ohana<sup>1</sup>, Yonatan Dolev<sup>1</sup>, Amir H. Tavabi<sup>2</sup>, Rafal E. Dunin-Borkowski<sup>2</sup>, Ido Kaminer<sup>1</sup>

<sup>1</sup>Technion – Israel Institute of Technology, Faculty of Electrical and Computer Engineering, Haifa, Israel

<sup>2</sup>Forschungszentrum Jülich GmbH, Ernst Ruska-Centre (ER-C), Jülich, Germany

<sup>3</sup>School of Physics, Trinity College Dublin, College Green, Dublin, Ireland

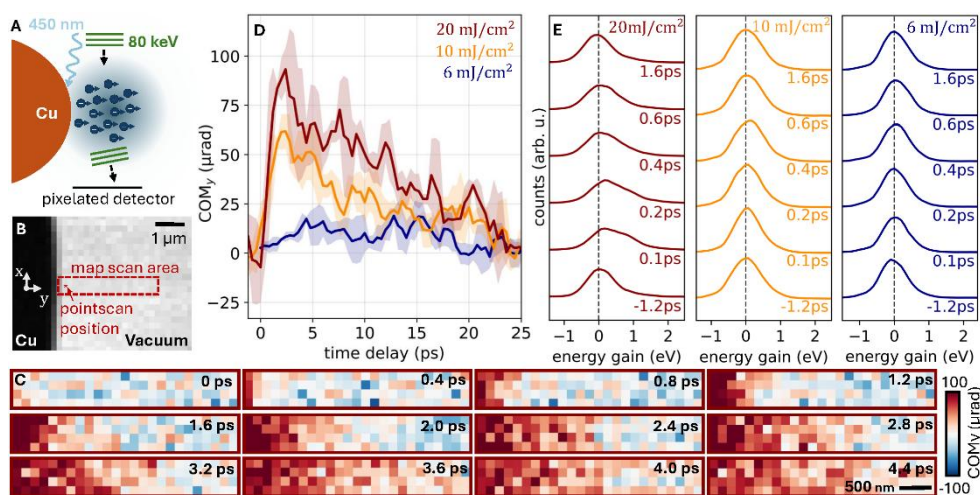
\*nicolai.b@campus.technion.ac.il

Understanding photoemission-driven charge dynamics at metal surfaces is important for the judicial design of electron sources and studies of ultrafast plasma formation. Following femtosecond laser excitation, transient electron clouds are formed and evolve collectively on femtosecond time scales, generating rapidly varying near-surface electric fields [1, 2].

Recently, the use of free-electron pulses in ultrafast TEM [1,2] and ultrafast SEM [3] was offered as means to probe photoemission dynamics, by measuring the inelastic or elastic scattering of the free-electrons of the photoemitted electron-cloud field. Despite these efforts, an accurate and complete spatio-temporal description of the intricate dynamics of photoemission is still missing. The challenge originates from the interplay of multi-electron Coulomb interactions on ultrafast timescales, occurring in a nanometric area near the surface. Previous approaches lacked the contrast to resolve the intricate features of this process due to the rapid decay of the charge-induced fields following electron cloud expansion.

Here, we present ultrafast 4D-STEM of photoemission dynamics, creating a spatiotemporal movie of the nano-plasma field via field-induced elastic beam deflections. We use a model photoemission system - a bulk Cu surface [1] (Fig. 1A and 1B). We further compare our approach to STEM-EELS (Fig. 1C-E), finding that 4D-STEM remains sensitive to photoemission dynamics at lower pump fluences and later time delays (25 ps vs. only 2 ps), persisting several micrometers from the surface and revealing the long-time charge-cloud evolution. This improved sensitivity likely reflects the fact that 4D-STEM directly probes the electric fields, whereas inelastic scattering is sensitive to the faster-decaying current density generated by the moving charges. These results suggest that ultrafast 4D-STEM can access intricate ultrafast dynamics down to individual charges and novel effects like carrier cooling.

**Fig. 1: Photoemission from a Cu surface probed by ultrafast 4D-STEM and compared with inelastic scattering.** (A) Experimental schematic. (B) Bright-field image of the Cu-vacuum edge. (C) Probe center-of-mass (COM) deflection normal to the surface (along y axis) at selected pump-probe delays for 20 mJ/cm<sup>2</sup> pump fluence. The ROI is marked by the frame in (B). (D) Temporal evolution of the COM deflection at the position marked in (B), for three pump fluences. (E) Corresponding inelastic scattering spectra, as in CDEM [1], measured at the same position and excitation conditions as in (D). Contrast is far less apparent compared to COM.



probe delays for 20 mJ/cm<sup>2</sup> pump fluence. The ROI is marked by the frame in (B). (D) Temporal evolution of the COM deflection at the position marked in (B), for three pump fluences. (E) Corresponding inelastic scattering spectra, as in CDEM [1], measured at the same position and excitation conditions as in (D). Contrast is far less apparent compared to COM.

## References:

- [1] Madan, I. *et al.* ACS Nano **17**, 3657 (2023); Yannai, M. *et al.* ACS Nano **17**, 3645 (2023).
- [2] Zandi, O. *et al.*, Nat. Commun. **11**, 3001 (2020).
- [3] Koutenský, P. *et al.*, ACS Photonics **12**, 4452 (2025).